# Kindlin-2 (Mig-2): a co-activator of $\beta_3$ integrins

Yan-Qing Ma,[1] Jun Qin,[1] Chuanyue Wu,[2] and Edward F. Plow[1]

[1]Department of Molecular Cardiology, Cleveland Clinic, Cleveland, OH 44195
[2]Department of Pathology, University of Pittsburgh School of Medicine, Pittsburgh, PA 15261

Integrin activation is essential for dynamically linking the extracellular environment and cytoskeletal/signaling networks. Activation is controlled by integrins' short cytoplasmic tails (CTs). It is widely accepted that the head domain of talin (talin-H) can mediate integrin activation by binding to two sites in integrin β's CT; in integrin $\beta_3$ this is an NPLY$^{747}$ motif and the membrane-proximal region. Here, we show that the C-terminal region of integrin $\beta_3$ CT, composed of a conserved TS$^{752}$T region and NITY$^{759}$ motif, supports integrin activation by binding to a cytosolic binding partner, kindlin-2, a widely distributed PTB domain protein. Co-transfection of kindlin-2 with talin-H results in a synergistic enhancement of integrin $\alpha_{IIb}\beta_3$ activation. Furthermore, siRNA knockdown of endogenous kindlin-2 impairs talin-induced $\alpha_{IIb}\beta_3$ activation in transfected CHO cells and blunts $\alpha_v\beta_3$-mediated adhesion and migration of endothelial cells. Our results thus identify kindlin-2 as a novel regulator of integrin activation; it functions as a coactivator.

## Introduction

Integrin activation, the rapid transition from a low to a high affinity state for ligand, regulates the numerous cellular responses consequent to integrin engagement by extracellular matrix proteins or counter-receptors on other cells (Hynes, 2002). This transformation is tightly controlled by the integrin cytoplasmic tails (CTs) (Qin et al., 2004; Ma et al., 2007). Mutational and structural analyses suggest that the $\beta_3$ CT can be divided two regions, and both influence integrin activation. The membrane-proximal region of the $\beta_3$ CT is primarily α-helix, which interacts with the membrane-proximal helix of the α subunit through several electrostatic and hydrophobic bonds (Vinogradova et al., 2002). Unclasping of the complex is a critical event in integrin activation (Hughes et al., 1996; Kim et al., 2003; Ma et al., 2006). The membrane-distal region of the $\beta_3$ CT contains two NXXY turn motifs, NPLY$^{747}$ and NITY$^{759}$, which are separated by a short helix containing a T/S cluster, the TS$^{752}$T region (Fig. 1 A). The head domain of talin (talin-H) docks at the NPLY$^{747}$ motif through its $F_3$ domain and also interacts with the membrane-proximal region, perturbing the membrane clasp and leading to at least partial integrin activation (Vinogradova et al., 2002; Tadokoro et al., 2003; Wegener et al., 2007). The T/S cluster and the NITY motif are also critical for integrin activation (Chen et al., 1994; O'Toole et al., 1995; Xi et al., 2003; Ma et al., 2006). However, the mechanisms underlying their effects remain unresolved. In this study, we found that kindlin-2, a widely distributed PTB domain protein, interacts with the C terminus of $\beta_3$ CT at the TS$^{752}$T and NITY$^{759}$ motifs and markedly enhances talin-induced integrin activation. Thus, kindlin-2 is identified as a coactivator of integrins.

Correspondence to Edward F. Plow: plowe@ccf.org

Abbreviations used in this paper: CT, cytoplasmic tail; HUVEC, human umbilical vein endothelial cell; talin-H, talin head domain.

The online version of this paper contains supplemental material.

## Results and discussion

To address the functional significance of the membrane-distal region of the $\beta_3$ CT, we considered whether it might interact with intracellular regulator(s). A CHO cell line stably expressing $\alpha_{IIb}\beta_3$ was transfected with cDNAs encoding for wild-type or mutated $\beta_3$ CT based on the rationale that these expressed constructs would compete for integrin binding partners. A similar strategy had been used previously to screen the β CT binding partners essential for integrin activation (Fenczik et al., 1997). In our studies, these $\beta_3$ CT were expressed as chimeric constructs containing the extracellular domain of PSGL-1 so that expression levels of the various $\beta_3$ CT could be verified. As assessed by flow cytometry (FACS), PSGL-1 expression differed by less than 10%. The effects of the various $\beta_3$ CT on $\alpha_{IIb}\beta_3$-mediated cell spreading on immobilized fibrinogen were evaluated. Compared with cells expressing PSGL-1 alone, expression of the wild-type $\beta_3$CT chimera totally abolished $\alpha_{IIb}\beta_3$-mediated cell spreading (Fig. 1 B). As a specificity control, Y$^{747}$A mutation, which would interfere with talin binding, resulted in a loss of inhibitory activity. Other mutations in the membrane-distal region in $\beta_3$ CT chimera, S$^{752}$P and Y$^{759}$A, beyond the talin interactive sites and which perturb


The Rockefeller University Press $30.00
J. Cell Biol. Vol. 181 No. 3 439–446
www.jcb.org/cgi/doi/10.1083/jcb.200710196

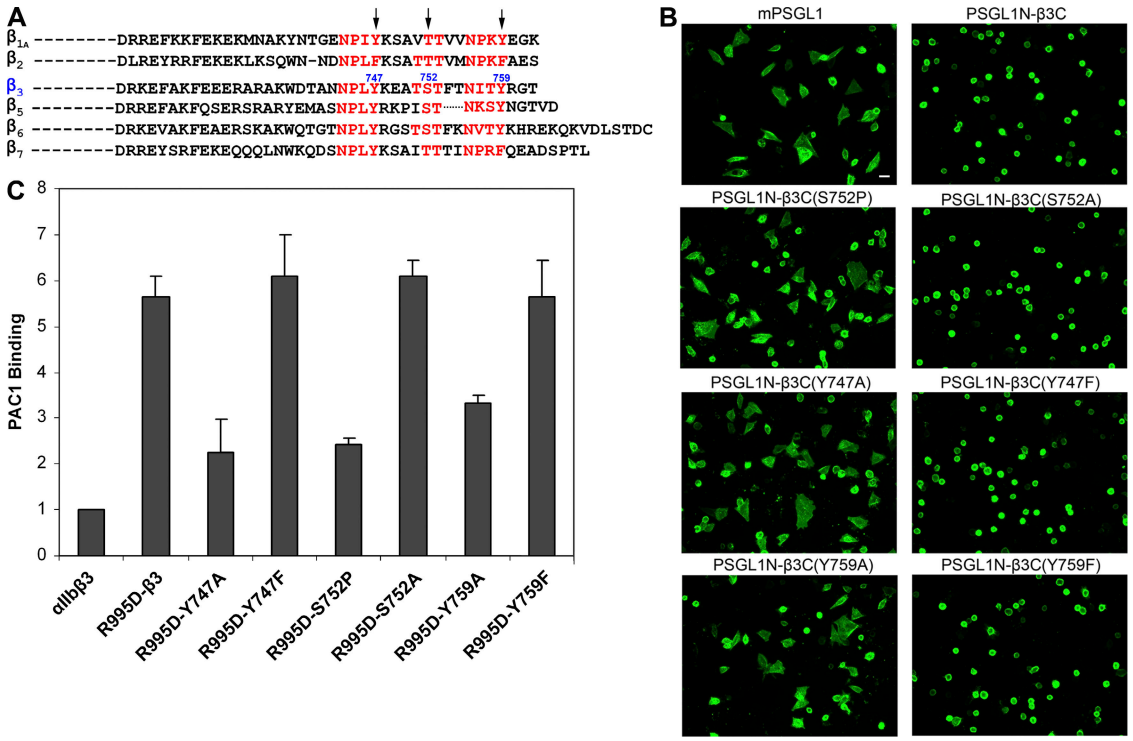


Figure 1. **Sequences of the membrane-distal region of $\beta_3$ CT have essential roles in integrin $\alpha_{IIb}\beta_3$ activation.** (A) Alignment of integrin β CT sequences, highlighting (red) the conserved regions, the two NXXY/F motifs and one T/S cluster. (B) Suppression of integrin $\alpha_{IIb}\beta_3$-mediated cell spreading by expressed $\beta_3$ CT depends on conserved sequences in its membrane-distal region. After transient transfection with plasmids encoding the indicated $\beta_3$ CT-containing chimera ($\beta_3$ CT/PSGL-1), adhesion of the $\alpha_{IIb}\beta_3$-CHO cells to fibrinogen was examined. The adherent cells were fixed and stained with the anti-PSGL-1 mAb, KPL-1, for visualization by fluorescence microscopy (10× objective). Bar, 20 μm. (C) Conserved residues in the membrane-distal region support $\alpha_{IIb}\beta_3$ activation. Plasmids encoding $\alpha_{IIb}$ and $\beta_3$ or its mutants were transiently transfected to CHO cells. The transfected cells were stained with 2G12 to assess $\alpha_{IIb}\beta_3$ expression or PAC1 to assess $\alpha_{IIb}\beta_3$ activation. FACS was used to measure the mean fluorescence intensity (MFI) of 2G12 or PAC1 binding, and relative MFI of PAC1 binding was normalized to integrin expression levels based on 2G12 staining (Ma et al., 2006). The error bars represent means ± SD of three independent experiments.

key structural features in this region, the short helix and the turn motif, respectively, also led to loss of competitive activity. This loss was not observed with $Y^{747}F$, $S^{752}A$, or $Y^{759}F$ substitutions, which would sustain the secondary structural features of the membrane-distal region.

Cell spreading is a complex response and we sought to confirm the role of membrane-distal residues in integrin activation more directly. $\alpha_{IIb}\beta_3$ containing a point mutation of $R^{995}D$ in $\alpha_{IIb}$ or $D^{723}R$ in $\beta_3$, which disrupts a salt bridge formed by $R^{995}$ and $D^{723}$, is a particularly sensitive reporter of talin-H–induced activation in a CHO cell system as assessed with the ligand mimetic mAb, PAC1 (Hughes et al., 1996; Tadokoro et al., 2003; Ma et al., 2006). Disrupting either of the two NXXY turn motifs, $NPLY^{747}$ or $NITY^{759}$, with a $Y^{747}A$ or a $Y^{759}A$ mutation dramatically impairs integrin activation caused by $R^{995}D$ (Fig. 1 C). However, conservative substitutions that should be structurally silent, $Y^{747}F$ or $Y^{759}F$, have no significant effect on integrin activation. Consistent with previous data, disruption of the short helix between two NXXY motifs with the naturally occurring $S^{752}P$ (Chen et al., 1992, 1994) suppresses integrin activation whereas the $S^{752}A$ substitution, which maintains the helix (Ma et al., 2006), does not affect activation. Although the above description focuses on the $\beta_3$ CT, most of the key sequences are shared by other integrin β subunits (Fig. 1 A), and the potential to be activated extends to multiple integrin subfamilies.

A reasonable synthesis of the data in Fig. 1 (B and C) is that the membrane-distal region of the $\beta_3$ CT regulates integrin activation and does so by interacting with a cytoplasmic binding partner that cooperates with talin but binds to distinct sites. Molecules reported to bind to the membrane-distal conservative regions of $\beta_3$ CT include filamin, which binds to the T/S cluster, and $\beta_3$-endonexin, which binds to the $NITY^{759}$ motif. Both have been suggested as regulators of integrin activation (filamin, a negative regulator, and $\beta_3$-endonexin, a positive regulator) (Eigenthaler et al., 1997; Kiema et al., 2006). To assess their roles in integrin activation, filamin A Ig-like domain 21 (FLNa21, the β CT binding region) or $\beta_3$-endonexin was transfected or cotransfected together with talin-H into $\alpha_{IIb}\beta_3$-CHO cells. Neither modulated talin-induced integrin activation or directly mediated integrin activation (Fig. 2, A and B; and Fig. S1 A, available at http://www.jcb.org/cgi/content/full/jcb.200710196/DC1), thus excluding them as the hypothetical coactivator of integrins. It should be noted that these data are not inconsistent with the proposed role of filamin A as a negative regulator of integrin activation (Kiema et al., 2006); suppressive effects of FLNa21 may not be evident in the presence of high talin-H levels.

Recently, we identified another $\beta_3$ CT binding protein, kindlin-2 (Shi et al., 2007), one of a three-member kindlin family that are characterized by bearing a FERM domain (Wick et al., 1994; Siegel et al., 2003; Weinstein et al., 2003; Ussar et al., 2006).

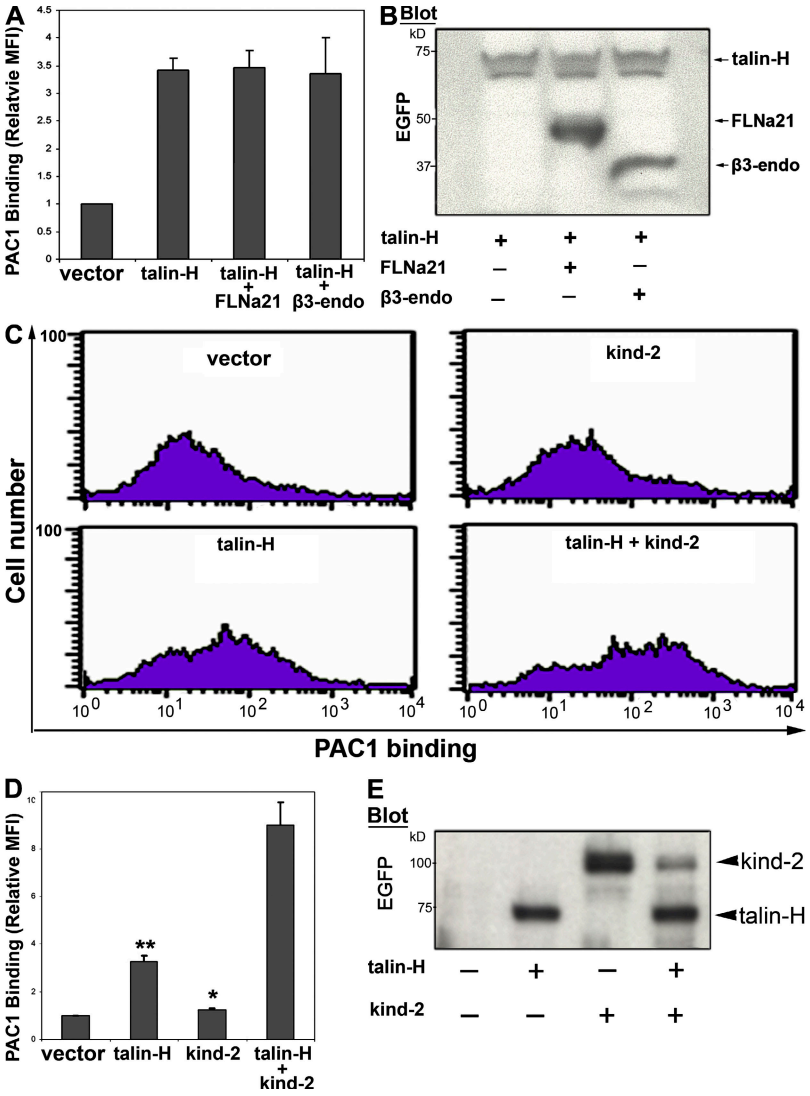


Figure 2. **Kindlin-2 enhances talin-induced integrin $\alpha_{IIb}\beta_3$ activation.** EGFP-fused $\beta_3$ CT binding proteins were transiently transfected into $\alpha_{IIb}\beta_3$-CHO cells. Their effects on $\alpha_{IIb}\beta_3$ activation were evaluated by PAC1 binding (A and D) and expression levels were measured by Western blotting with anti-GFP antibody (B and E). Representative FACS histograms of PAC1 binding to talin-H and/or kindin-2 (kind-2) positive cells (C). Error bars (A and D) represent means ± SD ($n$ = 3). *, $P < 0.05$; **, $P < 0.01$ (versus vector).

Kindlin-2 contributes to the maturation of focal adhesions during cell shape changes through recruitment of migfilin and filamin (Tu et al., 2003). Targeted disruption of the kindlin-2 gene results in embryonic lethality in mice and causes multiple, severe abnormalities in zebrafish (Dowling et al., 2008). Distinct from talin, its interaction site on $\beta_3$ CT is not dependent on the NPLY$^{747}$ motif (Shi et al., 2007). When expressed in $\alpha_{IIb}\beta_3$-CHO cells, kindlin-2 induces statistically significant but very weak integrin activation compared with talin-H (Shi et al., 2007). To consider the role of kindlin-2 a coactivator with talin-H, both were transfected into $\alpha_{IIb}\beta_3$-CHO cells. As shown in Fig. 2 (C and D), kindlin-2 dramatically enhanced talin-H–mediated $\alpha_{IIb}\beta_3$ activation. This enhancement was not simply additive but represented functional synergism. We assessed the expression levels in different transfectants by Western blots to exclude that coexpression of kindlin-2 enhanced talin-H expression or vise-versa; expression of talin-H in single and double transfectants was similar (Fig. 2 E).

To further assess the role of kindlin-2 as a coactivator, GST-fused $\beta_3$ CT proteins were used to coprecipitate endogeneous kindlin-2 in lysates of CHO cells, platelets, and human umbilical vein endothelial cells (HUVECs). As shown in Fig. 3 A, wild-type $\beta_3$ CT interacts with kindlin-2 but GST alone did not, ascribing specificity to the interactions. The Y$^{747}$A mutation abrogates talin-H but not kindin-2 binding to $\beta_3$ CT. In contrast, the S$^{752}$P and Y$^{759}$A mutations still support talin-H binding but dramatically reduce kindlin-2 association (Fig. 3 A). Thus, the binding requirements for talin-H and kindlin-2 on the $\beta_3$ CT are distinct and both bind to sites known to regulate integrin activation. Consistent with our observations (Fig. 2 A and Fig. S1 A), overexpression of FLNa21 or $\beta_3$-endonexin, two C-terminal binding proteins of $\beta_3$ CT, failed to suppress endogenous kindlin-2 binding to $\beta_3$ CT in CHO cells (Fig. S1 B), indicating a privileged interaction of kindlin-2 with the $\beta_3$ CT among these binding partners. As a point of emphasis, endogenous kindlin-2 coprecipitates with endogenous $\beta_3$ integrin subunit in both $\alpha_{IIb}\beta_3$-CHO cells and HUVECs (Fig. S2, available at http://www.jcb.org/cgi/content/full/jcb.200710196/DC1).

Peptides corresponding to Y$^{747}$-T$^{762}$ or a variant peptide containing the S$^{752}$P and Y$^{759}$A substitutions were synthesized (Fig. 3 B). When added as competitors (200 μM), wild-type Y$^{747}$-T$^{762}$ peptide inhibited kindlin-2 coprecipitation with the

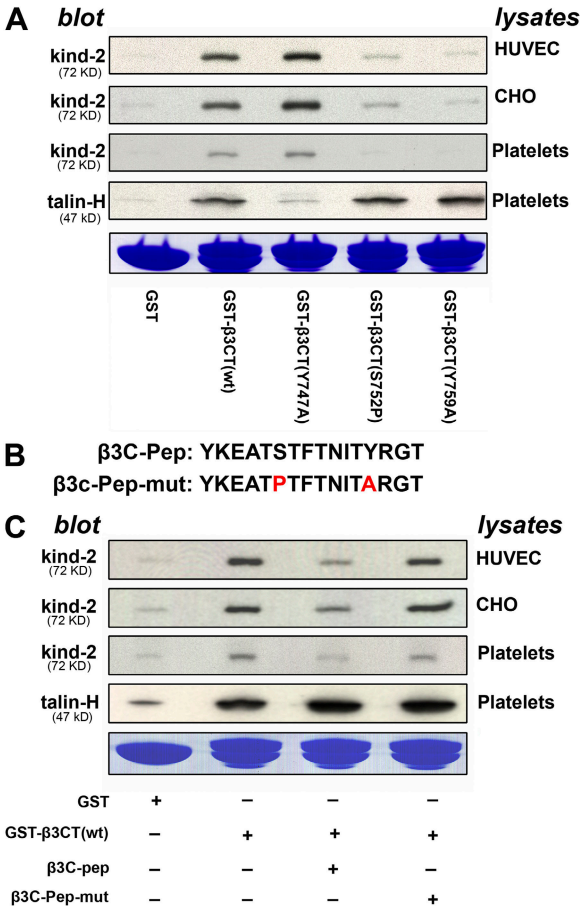


Figure 3. **Distinct binding sites for kindlin-2 and talin in $\beta_3$ CT.** (A) Lysates of CHO cells, HUVECs, or out-dated platelets were incubated with GST or GST-fused $\beta_3$ CT bearing the indicated mutations in the presence of glutathione-Sepharose. After washing, the precipitates were analyzed by SDS-PAGE. The loading of the GST proteins was assessed by Coomassie blue staining. The associated kindlin-2 or talin-H was detected in Western blots with anti-kindlin-2 or anti-talin-H. (B) Amino acid sequences of $\beta_3$ CT C-terminal peptide corresponding to $Y^{747}$-$T^{762}$ and a mutant peptide with two loss-of-function mutations, $S^{752}P$ and $Y^{759}A$. (C) The pull-down assay was performed in the presence of indicated peptides. The influence of these peptides on kindlin-2 or talin-H binding to $\beta_3$ CT was evaluated by SDS-PAGE and Western blotting.

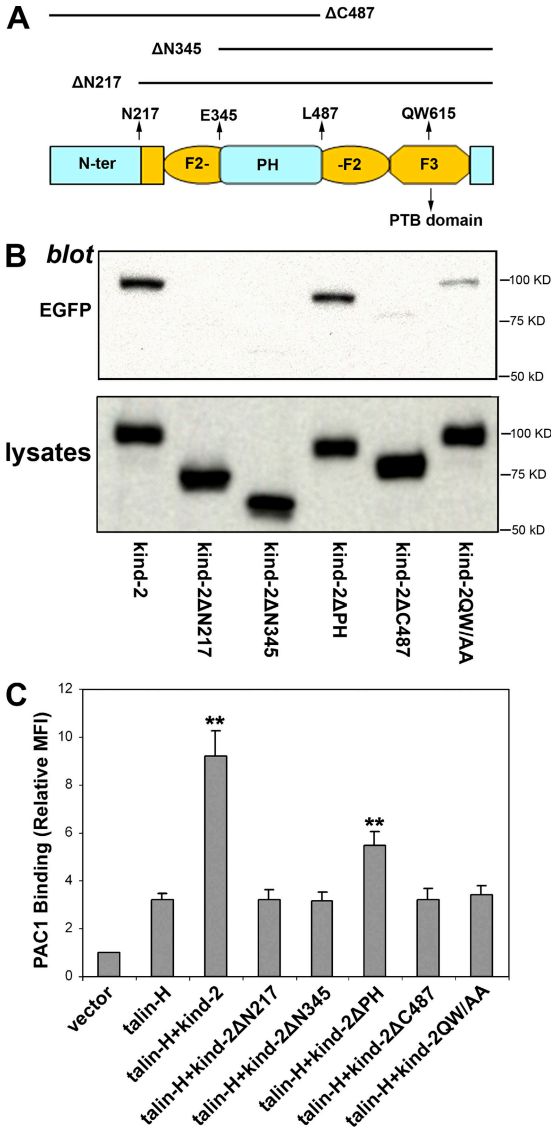


Figure 4. **Both the N and C terminus of kindlin-2 are required for $\beta_3$ CT association and support of talin-induced integrin activation.** (A) Organization of predicated domains of kindlin-2 protein. The FERM domain is shown in yellow, in which the $F_2$ subdomain is split by the PH domain. Deletion mutations from N terminus (ΔN) or C terminus (ΔC) are indicated. (B) The lysates of CHO cells transfected with EGFP-kindlin-2 with indicated mutations were used for pull-down assays. After incubating with GST fusion $\beta_3$ CT (wild-type) and glutathione-Sepharose, kindlin-2 protein bound to the $\beta_3$ CT was evaluated by SDS-PAGE and Western blotting using anti-GFP antibody. Kindlin-2 expression levels in lysates are also shown. (C) CHO cells expressing $\alpha_{IIb}\beta_3$ were transiently transfected with empty EGFP vector or cDNA encoding the indicated proteins. Binding of PAC1 to the different transfectants was assessed by FACS and relative MFI of PAC1 binding were calculated as described in Materials and methods. Error bars represent means ± SD ($n$ = 3). **, $P < 0.01$ (versus talin-H).

GST-$\beta_3$ CT (Fig. 3 C); the inhibition was ~70% by densitometry. A lower concentration of peptide (100 μM) was still inhibitory but produced only 50% inhibition (unpublished data), suggesting a dose-dependent inhibitory effect. Introduction of $S^{752}P$ and $Y^{759}A$ mutations into the peptide totally abolished its competitive activity (Fig. 3 C). As control, both peptides had no effect on talin-H association with the GST-$\beta_3$ CT. It is noteworthy that introduction of similar peptides into endothelial cells (Liu et al., 1996) and platelets (Hers et al., 2000) significantly perturbed $\alpha_v\beta_3$ and $\alpha_{IIb}\beta_3$ mediated responses, respectively. Thus, our results may provide a molecular explanation for these prior observations.

Like talin-H, kindlin-2 contains a FERM domain; its $F_2$ subdomain is bisected by a PH domain, but its $F_3$ (PTB) subdomain is intact (Fig. 4 A). Our previous experiments had shown that a $QW^{615}$/AA mutation in $F_3$, a site predicted by molecular modeling to be involved in β CT engagement, did, in fact, disrupt its association with β CT (Shi et al., 2007). We segmented kindlin-2 into several fragments, and their $\beta_3$ CT-binding capacities were evaluated by pull-down assays (Fig. 4 B). Deletion of the N-terminal region of kindlin-2, at N217 or at E345, the border of the PH domain insertion, ablated interaction with the $\beta_3$ CT. In addition, truncation of kindlin-2 to delete the second part of its $F_2$ and $F_3$ subdomains also disrupted $\beta_3$ CT interaction (Fig. 4 B). These deletions were more disruptive than the $QW^{615}$ mutation. However, with deletion of PH domain alone, the mutant

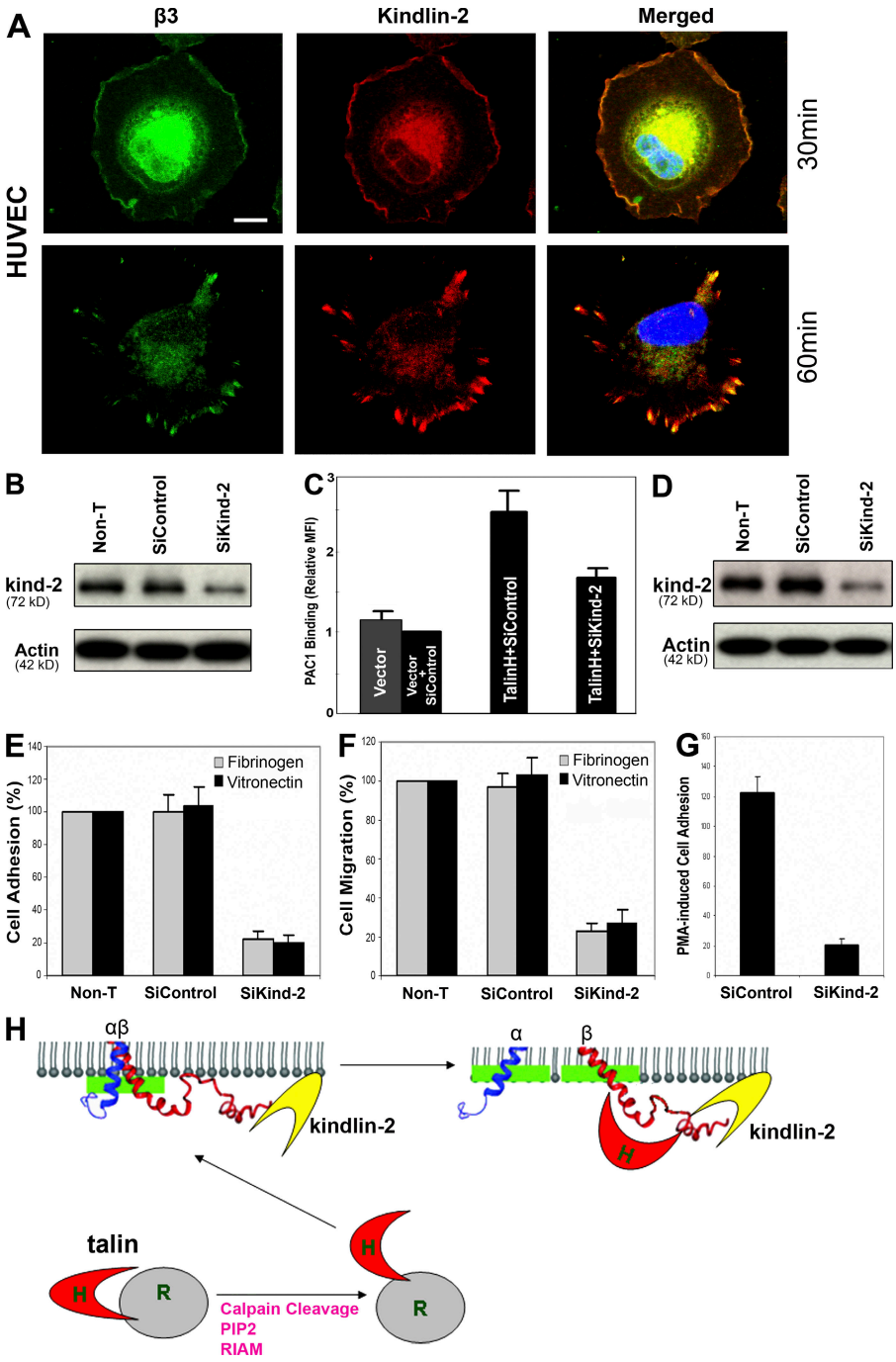


Figure 5. **Endogenous kindlin-2 supports $\beta_3$ integrin function in cells.** (A) Subcellular localizations of kindlin-2 and $\beta_3$ integrin. HUVECs spread on fibrinogen for 30 or 60 min were stained with the anti-kindlin-2 mAb and anti-$\beta_3$ subunit polyclonal antibody followed by Alexa-Fluor 568 anti–mouse IgG and AlexaFluor 488 anti–rabbit IgG. Bar, 10 μm. (B) RNAi suppression of kindlin-2 expression in CHO cells. Expression of kindlin-2 in parental CHO cells (non-T), kindlin-2 siRNA (SiKind-2), or control RNA (SiControl) transfectants was analyzed by Western blotting with kindlin-2 or actin antibodies. (C) CHO cells expressing $\alpha_{IIb}\beta_3$ were transiently transfected with vector or talin-H, together with control RNAs (SiControl) or siRNAs targeting kindlin-2 (SiKind-2). The binding of PAC1 to the different transfectants was assessed by FACS and MFI of PAC1 binding was calculated. The error bars are means ± SD ($n$ = 3). (D) RNAi suppression of kindlin-2 expression in HUVECs. (E and F) Non-transfected (Non-T) or HUVECs transfected with control RNAs (SiControl) or targeted siRNAs for Kindlin-2 (SiKind-2) were used in adhesion assays (E) or migration assays (F). The adherent or migrated cells were fixed, stained, and counted (10× objective). The error bars are means ± SD of three independent experiments. (G) HUVECs transfected with control RNAs (SiControl) or targeted siRNAs for kindlin-2 (SiKind-2) were stimulated with PMA, and adhesion to fibrinogen was measured. (H) Kindlin-2 as an integrin coactivator. Integrin activation depends on interaction of talin-H with the NPLY$^{747}$ motif and the membrane-proximal clasping region. Kindlin-2 facilitates activation by associating with the C-terminal regions of $\beta_3$ CT, involving the TS$^{752}$T and NITY$^{759}$ motifs.

kindlin-2 still retained its capacity to bind the $\beta_3$ CT. The effects of these mutants on the coactivator activity of kindlin-2 were tested. When cotransfected with talin-H, deletion of either the N- or C-terminal region of kindlin-2 resulted in loss of coactivator activity (Fig. 4 C). The mutant with its PH domain deletion still retained some coactivator activity, although it was less potent than intact kindlin-2. Also, the QW$^{615}$ mutant lacked coactivator activity, verifying that this site is involved not only in binding but also in coactivator function. We cannot exclude that some of these mutations may affect global folding of kindlin-2. However, it should be noted that FERM subdomains tend to fold independently into functional units. Thus, coactivator activity appears to depend on binding of kindlin-2 through both its N- and C-terminal $F_3$ (PTB) domains. As to why the C-terminal $F_3$ (PTB) of kindlin-2 recognizes the NITY$^{759}$ rather than the NPLY$^{747}$ region of $\beta_3$ CT will require high resolution structures.

The colocalization of $\beta_3$ integrin and kindlin-2 was also tested in living cells. We found they dynamically associate with each other in HUVECs during $\beta_3$ integrin mediated cell spreading on the $\beta_3$ ligand (Fig. 5 A). At the early stage of spreading (30 min), $\beta_3$ (green) and kindlin-2 (red) colocalized in the lamellipodia at the edges of spreading cells (Fig. 5 A, top). Over time, both $\beta_3$ integrin and kindlin-2 moved into focal adhesion sites (Fig. 5 A, bottom, 60 min). The merged images in Fig. 5 A (right)

verify the colocalization of kindlin-2 and $\beta_3$ integrin. $\beta_3$ integrin and talin also colocalize in spreading HUVECs with a similar pattern (Fig. S3 A, available at http://www.jcb.org/cgi/content/full/jcb.200710196/DC1). These observations place talin and kindlin-2 together, consistent with their cooperativity in function.

To determine if endogenous kindlin-2 supports $\beta_3$ integrin function, RNA-mediated interference experiments were performed. Small interfering RNAs targeting kindlin-2 (siKind-2) or irrelevant RNAs as control (siControl) were introduced into $\alpha_{IIb}\beta_3$-CHO cells, and kindlin-2 expression levels were analyzed by Western blot. Transfection of siKind-2 but not siControl effectively inhibited the expression of kindlin-2 (Fig. 5 B). The decrease in kindlin-2 protein expression was 70% by densitometry. Neither the siKind-2 nor the siControl changed actin expression, establishing selectivity of the siKind-2 on kindlin-2 expression. Talin-H can induce $\alpha_{IIb}\beta_3$ activation in transfected $\alpha_{IIb}\beta_3$-CHO cells as shown by others (Tadokoro et al., 2003) and in this study. However, talin-H–mediated integrin activation was significantly blunted when kindlin-2 levels were reduced with siKind-2 but not siControl (Fig. 5 C), indicating that endogenous kindlin-2 supports talin-H–induced $\alpha_{IIb}\beta_3$ activation in these cells.

We also tested the function of kindlin-2 knock-down in cells that express an integrin naturally. HUVECs express and use $\alpha_v\beta_3$ to mediate cell adhesion and migration on fibrinogen or vitronectin (Plow et al., 2000). Endogenous kindlin-2 could be knocked down in HUVEC using siRNA (Fig. 5 D), and the deficiency of kindlin-2 dramatically suppressed HUVEC adhesion on the $\beta_3$ integrin ligands, fibrinogen or vitronectin (Fig. 5 E). In addition, knockdown of kindlin-2 in HUVECs significantly inhibited VEGF-induced cell migration (Fig. 5 F). Under the conditions used, VEGF induced HUVEC migration on fibrinogen or vitronectin is dependent on $\alpha_v\beta_3$ activation (Byzova et al., 2000), and there is little cell proliferation (< 50% increase) in serum-free medium (unpublished data). Interestingly, we previously found that overexpression of kindlin-2 also inhibited migration for some cancer cells (Shi et al., 2007). These two distinct observations suggest that the supportive role of kindlin-2 in integrin activation might be cell type and/or integrin specific or depends on specific experimental conditions such as ligand concentration (Huttenlocher et al., 1996; Palecek et al., 1997). Furthermore, knocking down kindlin-2 significantly suppressed PMA-induced HUVEC adhesion on fibrinogen (Fig. 5 G), which is also an $\alpha_v\beta_3$ activation-dependent process. In concert, these results suggest that kindlin-2 plays an important role in supporting $\beta_3$ integrin functions dependent on activation.

Nonetheless, kindlin-2 is unlikely to be a direct activator of integrin; overexpression of kindlin-2 alone only had a mild effect on integrin activation compared with talin-H (Fig. 2 D). Even though kindlin-2 also bears a FERM-like domain as does talin-H, the binding sites of kindlin-2 on $\beta_3$ CT are solely localized at its C terminus beyond of the talin-H recognition sites (Fig. 3), which allows kindlin-2 and talin to bind to the $\beta_3$ CT together. This possibility has been established by the synergistic role of talin-H and kindlin-2 in integrin activation (Fig. 2, C and D) and further verified by the finding that knockdown of endogenous kindlin-2 significantly suppressed talin-H–induced integrin activation (Fig. 5, B and C).

In summary, we found that kindlin-2 is a coactivator of talin in supporting $\beta_3$ integrin activation. As such, kindlin-2 is the first of the postulated coactivators of integrins (Ma et al., 2007) to be identified. Our data support a model (Fig. 5 H) in which kindlin-2 binds to the C terminus of $\beta_3$ CT beyond of the talin-binding sites. Functionally, kindlin-2 synergistically enhances talin-induced integrin activation. Kindlin-2 may associate with membrane via its PH domain, an interaction commonly associated with these domains, and interacts with $\beta_3$ CT via its N terminus and C-terminal PTB domain. Anchoring $\beta_3$ CT by kindlin-2 could reduce the flexibility of $\beta_3$ CT in the cytosol, positioning it more favorably for interaction with talin and might also displace other $\beta_3$ CT binding partners. Due to the variable expression of kindlin-2 in different tissues and cells, e.g., its levels are quite low in human platelets versus HUVECs (Fig. S3 B), one must consider the possibilities that kindlin-2 may exert a "catalytic" effect on integrin activation, where one molecule coactivates multiple integrins, or whether this coactivator activity of kindlin-2 is shared or compensated by other kindlin family members or by other integrin binding partners.

## Materials and methods

### Plasmid construction and mutagenesis

The cDNA of human $\alpha_{IIb}$ and $\beta_3$ subunits were inserted into the mammalian expression vector pcDNA3.1 (Invitrogen). The mouse talin head domain (1–429 amino acids), human kindlin-2, $\beta_3$-endonexin, and filamin A Ig-like domain 21 (2235–2330 amino acids) were cloned into pEGFP vectors (Clontech Laboratories, Inc.). For the construct of GST-tagged $\beta_3$ cytoplasmic tail, the fragment of $\beta_3$ tail (716–762 amino acids) was amplified by PCR and inserted into pGST-parallel-1 vector (Sheffield et al., 1999). The PSGL-1/$\beta_3$ chimera was constructed in pcDNA3.1 vector in which N terminus (1–91 amino acids) of human PSGL-1 was fused onto C terminus (468–762 amino acids) of human $\beta_3$ subunit. All the indicated mutations were introduced into the respective constructs using QuikChange site-directed mutagenesis kit (Stratagene) and confirmed by gene sequencing.

### Integrin $\alpha_{IIb}\beta_3$ activation assay

The integrin $\alpha_{IIb}\beta_3$ activation was evaluated with PAC1, a mAb which specifically recognizes active $\alpha_{IIb}\beta_3$. For testing how the membrane-distal regions of $\beta_3$ CT regulate $\alpha_{IIb}\beta_3$ activation, the $\beta_3$ subunit bearing different mutations was cotransfected with $\alpha_{IIb}$ subunit, with or without $R^{995}D$ mutation, into CHO-K1 cells using Lipofectamine 2000 (Invitrogen). 24 h after transfection, the cells were collected and PAC1 binding was assessed as described previously (Ma et al., 2006). In brief, PAC1 binding was first normalized by $\alpha_{IIb}\beta_3$ expression level on the cell surfaces measured by mAb 2G12, which is against $\alpha_{IIb}\beta_3$ complex independent of activation status. The values of normalized PAC1 binding on different transfectants were compared to determine relative integrin activation, defining the basal activation of wild-type $\alpha_{IIb}\beta_3$ as 1.0.

For determining the regulatory roles of different $\beta_3$-binding partners in $\alpha_{IIb}\beta_3$ activation, individual EGFP-fused candidate binding partners or combinations of binding partners were transfected into CHO cells stably expressing wild-type $\alpha_{IIb}\beta_3$ ($\alpha_{IIb}\beta_3$-CHO). PAC1 binding to the different transfectants was analyzed by flow cytometry, gating only on the EGFP-positive cells. Mean fluorescence intensities (MFI) of PAC1 binding were normalized based on the basal level of PAC1 binding to cells transfected with the EGFP vector alone to obtain relative MFI values.

### Cell spreading

Monomeric PSGL-1 (mPSGL-1) or PSGL-1/$\beta_3$ chimera (PSGL1N-$\beta_3$C) was transfected into $\alpha_{IIb}\beta_3$-CHO cells. The mPSGL-1 was obtained by substitution of a single extracellular cysteine at the junction of the transmembrane domain with A to disturb the disulfide bond essential for PSGL-1 homodimer formation (McEver and Cummings, 1997). The transiently transfected cells were allowed to adhere and spread on immobilized fibrinogen in Laboratory-Tek II chambers (Nalge Nunc International). After incubation at 37°C for 2 h,

the chambers were washed three times with PBS and the adherent cells were fixed by 4% paraformaldehyde. To identify PSGL-1–expressing cells, the fixed cells were stained by anti-PSGL-1 mAb, KPL-1 (BD Biosciences), followed by goat anti–mouse IgG conjugated with AlexaFluor 488 (Invitrogen). As controls, nontransfected cells with the same treatment were included in each experiment and always showed no PSGL-1 staining. The positively stained (green) cells were observed using a fluorescence microscope (model DMR; Leica) with a 10X objective and recorded with a cooled CCD camera (Retiga Exi; Q-Imaging). Data were analyzed with ImagePro Plus Capture and Analysis software (Media Cybernetics).

### GST pull-down assays and Western blotting

Glutathione-*S*-transferase (GST) fusion proteins were expressed in Rosetta2 (DE3) cells, purified by glutathione-affinity chromatography using a GST-PrepFF column (GE Healthcare), and quantified by spectrophotometry using calculated extinction coefficients and Coomassie blue staining of SDS-PAGE. The cell lysates of transfected CHO cells, out-dated platelets, and HUVECs were prepared in the lysis buffer (50 mM Tris-HCl, pH 7.4, 150 mM NaCl, and 1% Triton X-100) containing protease inhibitors and centrifuged at 15,000 *g* for 12 min. For the GST pull-down assays, glutathione-Sepharose 4B (GE Healthcare) and the indicated GST fusion proteins were added to the aliquots of lysate supernatants and incubated at 4°C for 8 h. The antibodies used for Western blotting were anti-kindlin-2 (Tu et al., 2003), anti-GFP (Santa Cruz Biotechnology, Inc.), and anti–human talin (Chemicon International).

### Immunofluorescence and confocal microscopy

To observe the distributions of kindlin-2 and $\beta_3$ integrins, HUVECs were allowed to spread on immobilized fibrinogen at 37°C for 30 min or 60 min. The spread cells were fixed with 4% paraformaldehyde, permeabilized with 0.1% Triton X-100, and stained with mAb anti-kindlin-2 and polyclonal Ab anti-$\beta_3$ (Chemicon International) followed by AlexaFluor 568 anti–mouse IgG and AlexaFluor 488 anti–rabbit IgG (Invitrogen). The images were recorded by a confocal microscope with a 63X objective (Leica).

### RNA interference

To knock down endogenous kindlin-2, irrelevant control RNAs or designed siRNAs targeting kindlin-2 (from Dharmacon) were transfected to CHO cells using Lipofectamine 2000 (based on the protocol for siRNA transfection from Invitrogen) and HUVECs using targetfect-HUVEC (Targeting Systems) according to the manufacturers' protocols. The extent of suppression and specificity for kindlin-2 were evaluated by Western blotting with anti-kindlin-2 and actin antibodies as controls.

### HUVEC adhesion and migration

For cell adhesion assays, the nontransfected or transfected HUVECs, with targeting or control siRNAs, were incubated with the immobilized integrin ligand, fibrinogen (20 µg/ml for coating) or vitronectin (5 µg/ml for coating), for 30 min at 37°C. After washing, the adhered cells were fixed by 70% methanol and stained with 1% totuidine blue, and the cell number was counted under a microscope in several randomly selected fields. To test the effect of kindlin-2 deficiency on integrin $\alpha_v\beta_3$ activation, we stimulated transfected HUVECs with PMA and measured cell adhesion as previously described (Byzova et al., 2000). The PMA-induced cell adhesion was calculated as the increase based on the background without PMA treatment. Cell migration was performed in Transwell plates (8 µm pore size). In brief, the HUVEC suspensions were added to the upper chamber, which was precoated with fibrinogen or vitronectin and allowed to migrate for 8–12 h in the presence of 20 ng/ml recombinant human VEGF (R&D Systems) at 37°C in a 5% $CO_2$ humidified incubator. After migration, the cells on the upper surface of the filter were removed; and the migrated cells on the bottom surface of the filter were fixed with methanol, stained with 1% totuidine blue, and quantified by performing microscopic cell counts.

### Statistic analysis

Quantitative data were compared using a two-tailed *t* test. P values to determine statistical significance are indicated in the text. For the experiments to observe adherent or migrated cells, 10–20 fields or confocal cell images were randomly taken in at least three independent experiments.

### Online supplemental material

Fig. S1 shows that neither FLNa21 nor $\beta_3$-endonexin has direct effect on integrin $\alpha_{IIb}\beta_3$ activation and $\beta_3$ CT/kindlin-2 association. Fig. S2 shows the interaction of endogenous $\beta_3$ integrin subunit and kindlin-2. Fig. S3 shows the dynamic colocalization of $\beta_3$ integrin and talin in HUVECs and kindlin-2 expression in human platelets. Online supplemental material is available at http://www.jcb.org/cgi/content/full/jcb.200710196/DC1.

We thank Ka Chen, Zhen Xu, Kamila Bledzka, and Mitali Das for technical assistance.

This work was supported by NIH grants P01HL073311 (to E.F. Plow and J. Qin), GM62823 (to J. Qin), and GM65188 to C. Wu.

Submitted: 29 October 2007
Accepted: 1 April 2008

## References

Byzova, T.V., C.K. Goldman, N. Pampori, K.A. Thomas, A. Bett, S.J. Shattil, and E.F. Plow. 2000. A mechanism for modulation of cellular responses to VEGF: activation of the integrins. *Mol. Cell.* 6:851–860.

Chen, Y.-P., I. Djaffar, D. Pidard, B. Steiner, A.-M. Cieutat, J.P. Caen, and J.-P. Rosa. 1992. Ser-752→Pro mutation in the cytoplasmic domain of integrin $\beta_3$ subunit and defective activation of platelet integrin $\alpha_{IIb}\beta_3$ (GPIIb-IIIa) in a variant of Glanzmann's thrombasthenia. *Proc. Natl. Acad. Sci. USA.* 89:10169–10173.

Chen, Y.P., T.E. O'Toole, J. Ylanne, J.P. Rosa, and M.H. Ginsberg. 1994. A point mutation in the integrin beta 3 cytoplasmic domain (S752→P) impairs bidirectional signaling through alpha IIb beta 3 (platelet glycoprotein IIb-IIIa). *Blood.* 84:1857–1865.

Dowling, J.J., E. Gibbs, M. Russell, D. Goldman, J. Minarcik, J.A. Golden, and E.L. Feldman. 2008. Kindlin-2 is an essential component of intercalated discs and is required for vertebrate cardiac structure and function. *Circ. Res.* 102:423–431.

Eigenthaler, M., L. Hofferer, S.J. Shattil, and M.H. Ginsberg. 1997. A conserved sequence motif in the integrin beta3 cytoplasmic domain is required for its specific interaction with beta3-endonexin. *J. Biol. Chem.* 272:7693–7698.

Fenczik, C.A., T. Sethi, J.W. Ramos, P.E. Hughes, and M.H. Ginsberg. 1997. Complementation of dominant suppression implicates CD98 in integrin activation. *Nature.* 390:81–85.

Hers, I., J. Donath, P.E.M.H. Litjens, G. Van Willigen, and J.W.N. Akkerman. 2000. Inhibition of platelet integrin $\alpha_{IIb}\beta_3$ by peptides that interfere with protein kinases and the $\beta_3$ tail. *Arterioscler. Thromb. Vasc. Biol.* 20:1651–1660.

Hughes, P.E., F. Diaz-Gonzalez, L. Leong, C. Wu, J.A. McDonald, S.J. Shattil, and M.H. Ginsberg. 1996. Breaking the integrin hinge. A defined structural constraint regulates integrin signaling. *J. Biol. Chem.* 271:6571–6574.

Huttenlocher, A., M.A. Ginsberg, and A.F. Horwitz. 1996. Modulation of cell migration by integrin-mediated cytoskeletal linkages and ligand-binding affinity. *J. Cell Biol.* 134:1551–1562.

Hynes, R.O. 2002. Integrins: bidirectional, allosteric signaling machines. *Cell.* 110:673–687.

Kiema, T., Y. Lad, P. Jiang, C.L. Oxley, M. Baldassarre, K.L. Wegener, I.D. Campbell, J. Ylanne, and D.A. Calderwood. 2006. The molecular basis of filamin binding to integrins and competition with talin. *Mol. Cell.* 21:337–347.

Kim, M., C.V. Carman, and T.A. Springer. 2003. Bidirectional transmembrane signaling by cytoplasmic domain separation in integrins. *Science.* 301:1720–1725.

Liu, K.Y., S. Timmons, and J. Hawiger. 1996. Identification of a functionally important sequence in the cytoplasmic tail of integrin $\beta_3$ by using cell-permeable peptide analogs. *Proc. Natl. Acad. Sci. USA.* 93:11819–11824.

Ma, Y.Q., J. Yang, M.M. Pesho, O. Vinogradova, J. Qin, and E.F. Plow. 2006. Regulation of integrin alpha(IIb)beta(3) activation by distinct regions of its cytoplasmic tails. *Biochemistry.* 45:6656–6662.

Ma, Y.Q., J. Qin, and E.F. Plow. 2007. Platelet integrin alpha(IIb)beta(3): activation mechanisms. *J. Thromb. Haemost.* 5:1345–1352.

McEver, R.P., and R.D. Cummings. 1997. Perspectives series: cell adhesion in vascular biology. Role of PSGL-1 binding to selectins in leukocyte recruitment. *J. Clin. Invest.* 100:485–491.

O'Toole, T.E., J. Ylanne, and B.M. Culley. 1995. Regulation of integrin affinity states through an NPXY motif in the β subunit cytoplasmic domain. *J. Biol. Chem.* 270:8553–8558.

Palecek, S.P., J.C. Loftus, M.H. Ginsberg, D.A. Lauffenburger, and A.F. Horwitz. 1997. Integrin-ligand binding properties govern cell migration speed through cell-substratum adhesiveness. *Nature.* 385:537–540.

Plow, E.F., T.A. Haas, L. Zhang, J. Loftus, and J.W. Smith. 2000. Ligand binding to integrins. *J. Biol. Chem.* 275:21785–21788.

Qin, J., O. Vinogradova, and E.F. Plow. 2004. Integrin bidirectional signaling: a molecular view. *PLoS Biol.* 2:e169.

Sheffield, P., S. Garrard, and Z. Derewenda. 1999. Overcoming expression and purification problems of RhoGDI using a family of "parallel" expression vectors. *Protein Expr. Purif.* 15:34–39.

Shi, X., Y.Q. Ma, Y. Tu, K. Chen, S. Wu, K. Fukuda, J. Qin, E.F. Plow, and C. Wu. 2007. The MIG-2/integrin interaction strengthens cell-matrix adhesion and modulates cell motility. *J. Biol. Chem.* 282:20455–20466.

Siegel, D.H., G.H. Ashton, H.G. Penagos, J.V. Lee, H.S. Feiler, K.C. Wilhelmsen, A.P. South, F.J. Smith, A.R. Prescott, V. Wessagowit, et al. 2003. Loss of kindlin-1, a human homolog of the *Caenorhabditis elegans* actin-extracellular-matrix linker protein UNC-112, causes Kindler syndrome. *Am. J. Hum. Genet.* 73:174–187.

Tadokoro, S., S.J. Shattil, K. Eto, V. Tai, R.C. Liddington, J. M.de Pereda, M.H. Ginsberg, and D.A. Calderwood. 2003. Talin binding to integrin β tails: a final common step in integrin activation. *Science.* 302:103–106.

Tu, Y., S. Wu, X. Shi, K. Chen, and C. Wu. 2003. Migfilin and Mig-2 link focal adhesions to filamin and the actin cytoskeleton and function in cell shape modulation. *Cell.* 113:37–47.

Ussar, S., H.V. Wang, S. Linder, R. Fassler, and M. Moser. 2006. The Kindlins: subcellular localization and expression during murine development. *Exp. Cell Res.* 312:3142–3151.

Vinogradova, O., A. Velyvis, A. Velyviene, B. Hu, T.A. Haas, E.F. Plow, and J. Qin. 2002. A structural mechanism of integrin αIIbß3 "inside-out" activation as regulated by its cytoplasmic face. *Cell.* 110:587–597.

Wegener, K.L., A.W. Partridge, J. Han, A.R. Pickford, R.C. Liddington, M.H. Ginsberg, and I.D. Campbell. 2007. Structural basis of integrin activation by talin. *Cell.* 128:171–182.

Weinstein, E.J., M. Bourner, R. Head, H. Zakeri, C. Bauer, and R. Mazzarella. 2003. URP1: a member of a novel family of PH and FERM domain-containing membrane-associated proteins is significantly over-expressed in lung and colon carcinomas. *Biochim. Biophys. Acta.* 1637:207–216.

Wick, M., C. Burger, S. Brusselbach, F.C. Lucibello, and R. Muller. 1994. Identification of serum-inducible genes: different patterns of gene regulation during G0→S and G1→S progression. *J. Cell Sci.* 107(Pt 3):preceding table of contents.

Xi, X., R.J. Bodnar, Z. Li, S.C. Lam, and X. Du. 2003. Critical roles for the COOH-terminal NITY and RGT sequences of the integrin beta3 cytoplasmic domain in inside-out and outside-in signaling. *J. Cell Biol.* 162:329–339.